A Narrow-Band Level-Set Method with Dynamic Velocity for Neural Stem Cell Cluster Segmentation

Nezamoddin N. Kachouie and Paul Fieguth

Department of Systems Design Engineering,
University of Waterloo, Waterloo, Canada
nnezamod@engmail.uwaterloo.ca
pfieguth@uwaterloo.ca
http://www.ocho.uwaterloo.ca

Abstract. Neural Stem Cells (NSCs) have a remarkable capacity to proliferate and differentiate to other cell types. This ability to differentiate to desirable phenotypes has motivated clinical interests, hence the interest here to segment Neural Stem Cell (NSC) clusters to locate the NSC clusters over time in a sequence of frames, and in turn to perform NSC cluster motion analysis. However the manual segmentation of such data is a tedious task. Thus, due to the increasing amount of cell data being collected, automated cell segmentation methods are highly desired. In this paper a novel level set based segmentation method is proposed to accomplish this segmentation. The method is initialization insensitive, making it an appropriate solution for automated segmentation systems. The proposed segmentation method has been successfully applied to NSC cluster segmentation.

1 Introduction

Neural Stem Cells (NSCs) as building blocks of the brain can proliferate and differentiate into all neural phenotypes. Progress in the analysis of NSC functional properties is required for development of clinically applicable procedures for stem cell transplantation and for the treatment of various incurable diseases. NSC can be used to repair damaged neuro-degenerative processes such as Alzheimer and to repair brain injuries such as stroke.

Due to the universal attributes of NSCs, there has been great interest to develop a practical automated approach to measure and extract NSCs properties from microscopic cell images and track individual cells over time. To accomplish this task the NSC clusters must first be segmented. In practice, due to the presence of clutter, corrupted and blurred images, manual cell segmentation is a tedious task. An automated cell segmentation system may eliminate the onerous process of manual cell segmentation, extracting cell features from microscopic images.

Several methods have been developed for region segmentation such as region growing, watershed and thresholding methods [2, 5]. Recently researchers have

M. Kamel and A. Campilho (Eds.): ICIAR 2005, LNCS 3656, pp. 1006–1013, 2005.

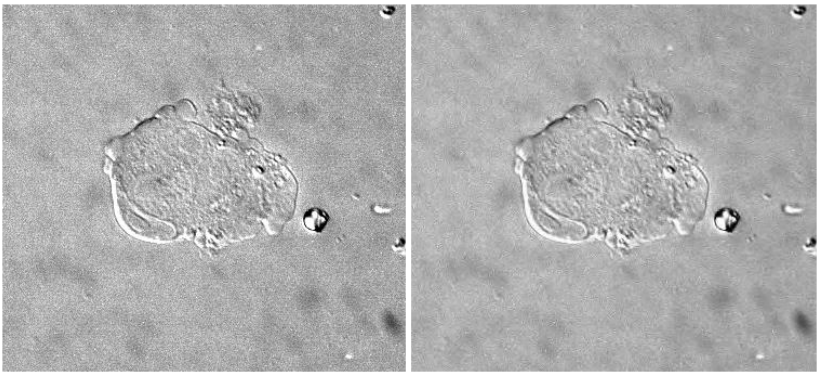

Fig. 1. (Left) Noisy NSC cluster image, (Right) Denoised image using BayesShrink Wavelet denoising

been more interested in deformable partitioning methods based on Partial Differential Equations (PDEs), as in deformable region segmentation by employing methods of snakes and level sets [6,7,8] In this paper a PDE-based cell segmentation method is presented to segment NSC Clusters.

2 Background: Level Set Method

Level sets were first introduced by Osher, Sethien and Malladi [6,7,9] for shape recovery. This framework supports problems from fluid mechanics to image processing [6], with image processing applications including segmentation, denoising, and restoration. The initial position of an interface is considered as the zero level set of a higher-dimensional surface. Implicitly representing the curve by the zero level set of a function has some major benefits in comparison with the explicit definition and evolution of the interface. These benefits can be summarized as topology independence and numerical stability to handle singularities. Since each level set surface has a uniform spacing and is defined over a discrete grid, all derivatives can be computed using finite difference approximations, hence the problem of discretizing doesn't occur with the level set representation, though it is an important concern with an explicit representation of the interface in other deformable models such as snakes.

Let $\wp(t)$ be a simple time dependent closed curve which is considered as the zero level set of a higher dimensional function $\Phi(x, y, t)$ [6,7,9]:

$$\wp(t) = \{(x, y) | \Phi(x, y, t) = 0\} \tag{1}$$

To initialize the interface, let the level set function $\Phi(x, y, t)$ be consider as a signed distance function:

$$\Phi(x, y, t) = z(x, y) \tag{2}$$

where $z(x, y)$ is the distance from the closest point on the interface $\wp(t)$ to the point (x, y) such that if the point is inside the interface the distance is negative,

for the points outside the curve, the distance z is positive and it is equal to zero for all the points lie on the interface:

$$\wp(t) = \{(x, y)|z(x, y) = 0\} \tag{3}$$

Having $\Phi(x, y, t) = 0$, for each point on the interface, the chain rule can be used to derive

$$\Phi_t + \nabla\Phi(x, y, t).(x, y)' = 0 \tag{4}$$

Let N be the outward normal:

$$\hat{N} = \frac{\nabla\Phi}{|\nabla\Phi|} \tag{5}$$

The velocity function F is in the same direction with outward normal direction and we have

$$(x, y)' = F\hat{N} = F\frac{\nabla\Phi}{|\nabla\Phi|} \tag{6}$$

which yields the evolution equation of the interface as

$$\Phi_t + F|\nabla\Phi| = 0 \tag{7}$$

where, $\Phi(x, y, t = 0)$ is known. By using the numerical solutions of hyperbolic conservation laws (7) can be approximated. The approximation may be obtained by defining a discrete grid in $x-y$ domain and replacing the temporal and spatial derivatives by finite differences. Assume (j, k) as the grid points and define a uniform spacing between the grid points, Φ^k_{jk} is the approximate solution for $\Phi(j, k, h\Delta t)$ in time step $h\Delta t$:

$$\frac{\Phi^{k+1}_{jk} - \Phi^k_{jk}}{\Delta t} + F|\nabla_{jk}\Phi^k_{jk}| = 0 \tag{8}$$

Here the forward difference is used to define the finite difference. The curvature of the interface at each point can be calculated using the divergence of the unit normal vector:

$$\aleph = \nabla.\frac{\nabla\Phi}{|\nabla\Phi|} = \left\{\frac{\Phi_{xx}\Phi_y^2 - 2\Phi_x\Phi_y\Phi_{xy} + \Phi_{yy}\Phi_x^2}{(\Phi_x^2 + \Phi_y^2)^{\frac{3}{2}}}\right\} \tag{9}$$

3 Materials

NSC samples must be extracted and processed before imaging. NSC sample preparation is two stage process consisting of

1. The extraction of NSCs from the mice, and
2. The processing and culturing of NSCs.

An NSC phase contrast image is depicted in Fig. 1. The cells were imaged using manual focusing through a 5X phase contrast objective using a digital camera (Sony XCD-900) connected to a PC computer by an IEEE 1394 connector. Images were acquired every three minutes. When a cell division was observed, the progeny were imaged at higher magnification using a 40X DIC objective.

4 Methods

Employing the level sets for NSC cluster boundary detection, (7) must be solved. To find a solution for (7), considering the Hamilton-Jacobi equation:

$$\Re(q) = F\sqrt{q^2} = f|q| \tag{10}$$

Thus (7) can be written as

$$\Phi_t + \Re(\nabla\Phi) = 0 \tag{11}$$

Let $\nabla\Phi = q$; using the hyperbolic conservation law we can conclude that

$$q_t + \nabla\Re(q) = 0 \tag{12}$$

By discretizing, this equation can be solved as

$$\Phi_{jk}^{k+1} = \Phi_{jk}^{k} - \Delta t\Re(\nabla\Phi) \tag{13}$$

where $\nabla\Phi$ is computed using finite differences. Let the velocity function be [6]

$$F = V_g(V_0 - \eta\aleph) \tag{14}$$

where $\aleph$ and η are curvature and curvature coefficients respectively, V_0 is a constant velocity coefficient and V_g is gradient based velocity term, we will have

$$\Phi_t + V_g(V_0 - \eta\aleph)|\nabla\Phi| = 0 \tag{15}$$

As the most important part of the solution, an appropriate velocity function F based on the application (an automatic segmentation system) and nature of phase contrast microscopic NSC images must be designed. The evolving interface must converge toward a cluster boundary and stop in its vicinity. F can be determined based on the specific features of the object such as the object's gray level intensity, its texture, specific shape, etc. Since cell clusters and the background have almost the same gray level intensities, the first and second order statistics of the cluster's intensity are not useful terms to be considered for velocity function definition. To segment the cluster boundary, texture information can be used to define the velocity function. A bank of Gabor filters was considered to derive the velocity function, but to achieve valuable texture features by Gabor filter bank a minimum number of four orientations and four radial frequencies are required that reach the number of extracted textured images to 16 for every single frame. Although this is a very moderate number of filtered images, the computational burden is too expensive for this approach to be considered as an applicable solution for a large number of images over time. Based on the cell cluster image properties, different velocity functions were considered and designed. The following approach uses a dynamic velocity function which satisfies the systems requirement and produces the best results according to the segmentation accuracy and time spent:

$\phi = \phi_{initalize}$
$V_I = |\nabla B(D_\beta[I])|$
$V_{\phi_{nb}} = |\nabla B(D_\beta[I]_{\phi_{nb}})|$
do
{
  if $(\mu\{V_{\phi_{nb}}\} > \mu\{V_I\})$ *then*
    $\phi^{k+1} = \phi^k + \Delta t\{|\nabla\phi|(\epsilon\aleph + 1)\}$
  else
    $\phi^{k+1} = \phi^k + \Delta t\{$
      $|\nabla\phi|(\epsilon\aleph - \exp(-\alpha|\nabla B(D_\beta[I])|))\}$

  $V_{\phi_{nb}^{k+1}} = |\nabla B(D_\beta[I]_{\phi_{nb}^{k+1}})|$
}
while$(\phi^{k+1} \neq \phi^k)$

BayesShrink Wavelet Denoising [10,11] ($D_\beta[I]$) is used to denoise cell image I and $B(D_\beta[I])$ is blurred version of the denoised image which is obtained using a Gaussian filter. Subscript (nb) shows that the gradient is calculated on a narrow band close to the zero level set. The mean μ of the gradient is computed over the image and on the narrow band of the zero level set as well. An important attribute of this velocity function is that it changes based on the location of interface and ensures that the zero level set is attracted toward the boundaries (edge locations) and stops in the vicinity of edges. In the proposed method, in each iteration the mean of gradient over a narrow band close to the zero level set ($\mu\{V_{\phi_{nb}}\}$) is computed. Level set deformations are based on its curvature as long as ($\mu\{V_{\phi_{nb}}\} > \mu\{V_I\}$) is satisfied. As soon as the zero level set contour passes the boundary of the cell cluster, ($\mu\{V_{\phi_{nb}}\} > \mu\{V_I\}$) is not valid anymore and the level set deforms based on gradient speed function ($exp(-\alpha|\nabla B(D_\beta[I])|)$) and its curvature. The deformations will continue until the zero level set stops on the boundary of the NSC cluster.

5 Results and Conclusions

Fig. 2 shows the the deformations of the level set toward cell cluster boundary. The circular initialized curve is depicted, followed by the interface after 20, 30, 40, 50 and 60 iterations in which the interface is deforming based on its curvature. After 70 iterations, Fig. 3, where the mean gradient of the narrow band level set is not anymore greater than the mean gradient of the image, the interface begins to shrink toward the cell cluster boundary with a velocity which has two terms. The first is a gradient-based term and the second curvature-based. As depicted in Fig. 4, the interface is converging to the cell cluster boundary in which the major velocity term is the gradient based function.

In this paper a novel level set method was presented for Embryonic Stem Cell cluster segmentation in Phase Contrast microscopy images. The proposed

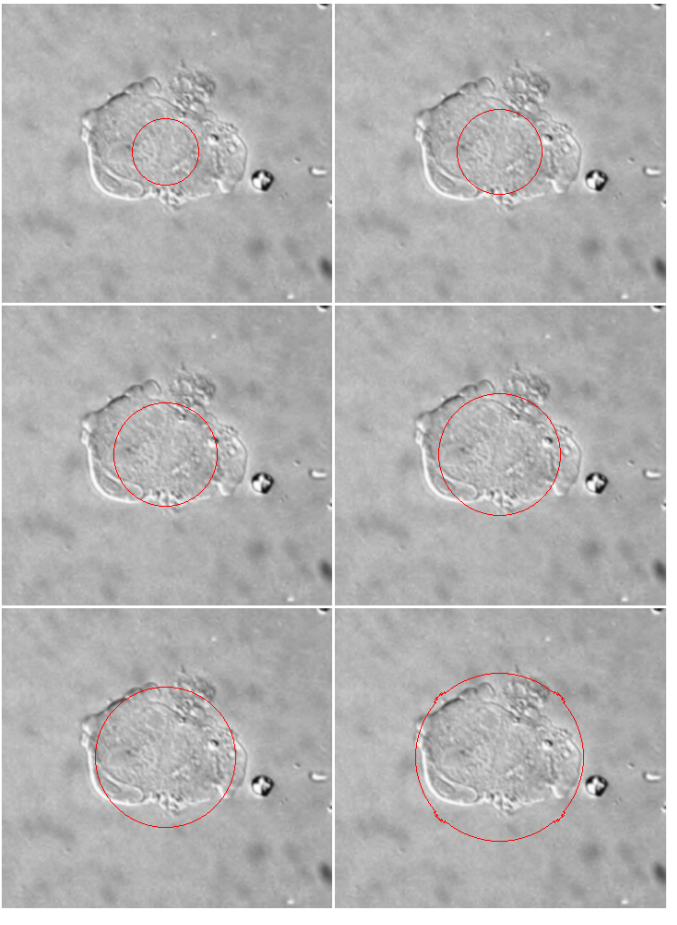

Fig. 2. The initialized curve (top left) and curvature based deformations after 20, 30, 40, 50 and 60 iterations

method is initialization insensitive and dynamically deforms toward cell cluster boundary. Hence it is an appropriate solution for automated segmentation systems. The proposed method is applied to NSC cluster image sequences and promising results are produced. Future work is to adapt the model to other cell types in the same category, extended in the form of coupled level sets with adaptive motion functions.

Acknowledgements

We would like to thank Dr. Eric Jervis and John Ramunas from the Chemical Engineering Department of the University of Waterloo for providing microscopic images for this research and their valuable comments on NSC biology, and Dr. Leo J. Lee for his valuable discussions on cell modelling.

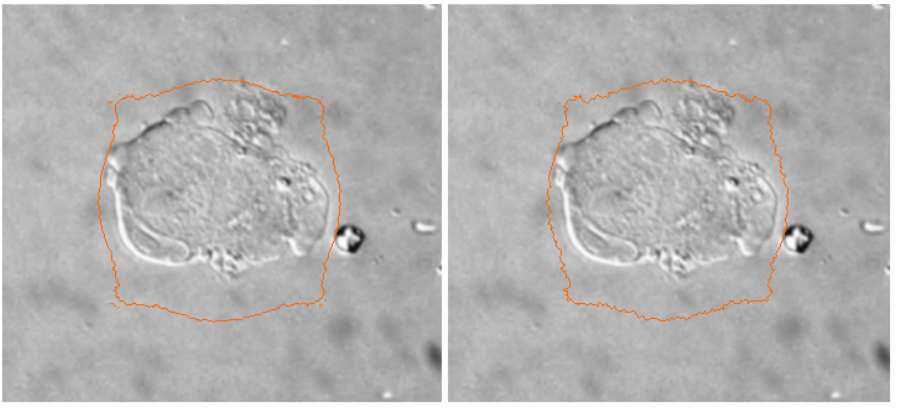

Fig. 3. Curvature based velocity function (left column) turns to gradient based velocity function (right column)

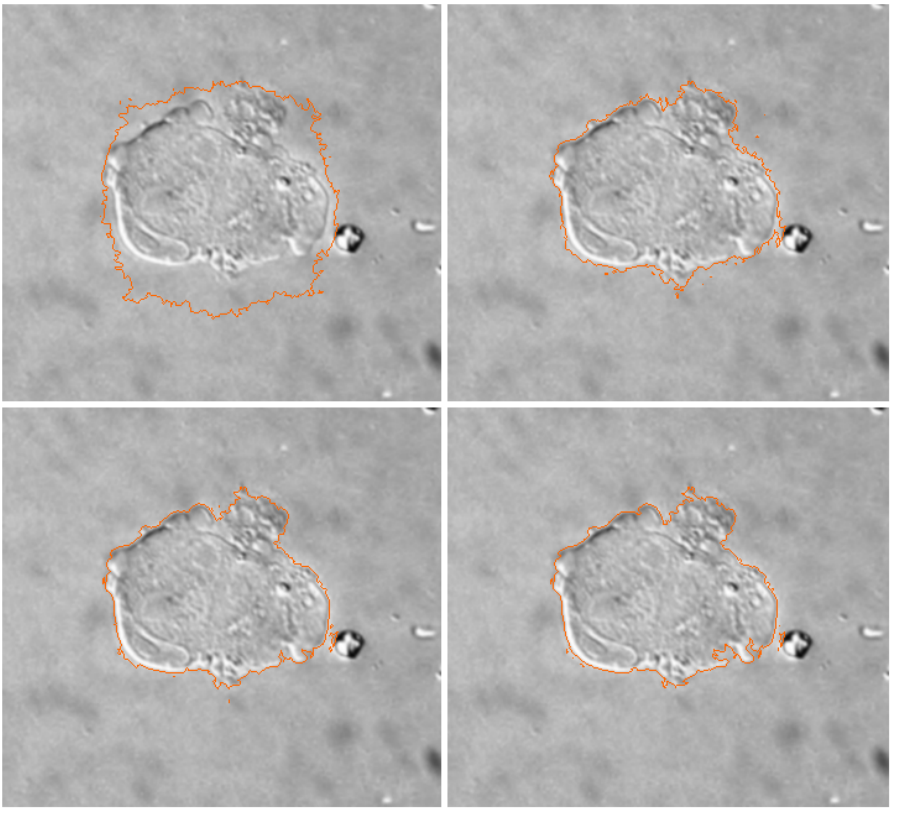

Fig. 4. Deforming curve based on gradient based velocity: First row and second row show the interface after 100, 200, 300 and 400 iterations where the cell boundary is completely segmented by the interface

References

1. G. Nistor, M. Totoiu, N. Haque, M. Carpenter, and H. Keirstead, "Human embryonic stem cells differentiate into oligodendrocytes in high purity and myelinate after spinal cord transplantation," *GLIA* **49**(3), pp. 385–396, 2004.
2. K. Wu, D. Gauthier, and M. Levine, "Live cell image segmentation," *IEEE Transactions on Biomedical Engineering* **42**(1), pp. 1–12, 1995.
3. J. Geusebroek, A. Smeulders, and F. Cornelissen, "Segmentation of cell clusters by nearest neighbour graphs," in *Proceedings of the third annual conference of the Advanced School for Computing and Imaging*, pp. 248–252, 1997.
4. T. Markiewicz, S. Osowski, L. Moszczyski, and R. Satat1, "Myelogenous leukemia cell image preprocessing for feature generation," in *5th International Workshop on Computational Methods in Electrical Engineering*, pp. 70–73, 2003.
5. D. Comaniciu and P. Meer, "Cell image segmentation for diagnostic pathology," *Advanced algorithmic approaches to medical image segmentation: State-of-the-art applications in cardiology, neurology, mammography and pathology* , pp. 541–558, 2001.
6. S. J. Osher and R. P. Fedkiw, *Level Set Methods and Dynamic Implicit Surfaces*, Springer, 2002.
7. J. Sethian, *Level Set Methods and Fast Marching Methods Evolving Interfaces in Computational Geometry, Fluid Mechanics, Computer Vision and Materials Science*, Cambridge University Press, 1999.
8. J. A. Yezzi, S. Kichenassamy, A. Kumar, P. Olver, and A. Tannenbaum, "A geometric snake model for segmentation of medical imagery," *IEEE Tran. on Medical Imaging* **16**(2), pp. 199–209, 1997.
9. R. Malladi, J. A. Sethian, and B. C. Vemuri, "Shape modeling with front propagation: A level set approach," *IEEE Transactions on PAMI* **27**(2), pp. 158–175, 1995.
10. D. L. Donoho and I. M. Johnstone, "Denoising by soft thresholding," *IEEE Tran. on Inf. Theory,* **41**, pp. 613–627, 1997.
11. S. G. Chang, B. Yu, and M. Vetterli, "Adaptive wavelet thresholding for image denoising and compression," *IEEE Trans. on Image Processing,* **9**(9), pp. 1532–1546, 2000.